

Turbulent front speed in the Fisher equation: Dependence on Damköhler numberAxel Brandenburg^{*}*NORDITA, AlbaNova University Center, Roslagstullsbacken 23, SE-10691 Stockholm, Sweden and
Department of Astronomy, Stockholm University, SE-10691 Stockholm, Sweden*Nils Erland L. Haugen[†]*Sintef Energy Research, N-7034 Trondheim, Norway*Natalia Babkovskaia[‡]*Division of Geophysics and Astronomy, P.O. Box 64, University of Helsinki, FI-00014 Helsinki, Finland
(Received 31 August 2010; published 11 January 2011)*

Direct numerical simulations and mean-field theory are used to model reactive front propagation in a turbulent medium. In the mean-field approach, memory effects of turbulent diffusion are taken into account to estimate the front speed in cases in which the Damköhler number is large. This effect is found to saturate the front speed to values comparable with the speed of the turbulent motions. By comparing with direct numerical simulations, it is found that the effective correlation time is much shorter than for nonreacting flows. The nonlinearity of the reaction term is found to make the front speed slightly faster.

DOI: [10.1103/PhysRevE.83.016304](https://doi.org/10.1103/PhysRevE.83.016304)

PACS number(s): 47.51.+a, 47.27.ek, 47.27.tb

I. INTRODUCTION

It is well known that the propagation speed of a flame front is greatly enhanced if a mixture of fuel and oxygen is in a turbulent state. This topic of turbulent premixed combustion was pioneered by Damköhler [1] some 70 years ago, and is reviewed extensively in recent literature [2–4]. In spite of its importance, the question of burning velocities in a turbulent medium continues to be of major importance even today [5–7].

Much of the current work is based on the original Damköhler paradigm for premixed combustion. He distinguishes two regimes, which are usually referred to as large-scale and small-scale turbulence. In the small-scale turbulence regime, also referred to as the distributed reaction zone regime, the turbulent flame speed is computed using a formula in which the microscopic diffusivity is replaced by the sum of microscopic and turbulent diffusivities. This is possible because there is good scale separation. This implies that the turbulent front thickness (i.e., the thickness of the flame brush) is much broader than the scale of the turbulent eddies. This regime is characterized by small Damköhler numbers. In the opposite case of large Damköhler numbers, the turbulent front thickness is smaller than the scale of the turbulent eddies and can therefore no longer be described by turbulent diffusion. This regime is characterized as that of large-scale turbulence. In this case, the turbulent front speed reaches its maximal value, which is given by the rms velocity of the turbulence in the direction of front propagation.

The regime of large-scale turbulence is subdivided further into regimes of corrugated and wrinkled flamelets, depending essentially on the ratio of Reynolds number to Damköhler number, which is also related to the Karlovitz number. When the Reynolds number is small compared with the Damköhler

number (small Karlovitz number), the flame front is merely wrinkled, but for large Reynolds numbers (large Karlovitz number) it becomes corrugated and can consist of isolated flamelets detached from other parts of the front. In the present paper, we will mainly be concerned with the flame speed rather than the question of whether the flame front is wrinkled or corrugated.

In turbulent combustion, the averaged flame speed, s_T , is usually normalized by the corresponding laminar flame speed, s_L , and one is interested in the dependence on the normalized turbulent velocity, v' . For the regime of large-scale turbulence, the speed-up ratio of turbulent to laminar flame speed is given by the geometric increase of the wrinkled surface area of the flame front. Damköhler assumed that the increase in surface area is proportional to the ratio of the turbulent velocity of the eddies to the laminar flame speed. This leads to the expectation that the dependence of s_T on v' is given by [2]

$$s_T/s_L = 1 + v'/s_L. \quad (1)$$

This equation captures the expected limiting cases that s_T should not become larger than v' for $v' \gg s_L$ and that $s_T = s_L$ in the absence of turbulence, that is, for $v' = 0$. However, unsatisfactory agreement with measurements motivated the search for other dependencies. For example, Pocheau [8] derives the more general formula

$$s_T/s_L = [1 + (v'/s_L)^n]^{1/n}, \quad (2)$$

where n is a parameter. This formula obeys the aforementioned limiting case for any value of n . Pocheau [8] contrasts the formula with another one proposed by Yakhot [9],

$$s_T/s_L = \exp[(v'/s_T)^2], \quad (3)$$

where $s_T < v'$ for $v' \rightarrow \infty$. Yet another fit formula is given by

$$s_T/s_L = 1 + C_W(v'/s_L)^m \quad (4)$$

with fit parameters C_W and $m = 0.7$ [10]. Both (3) and (4) have a front speed less than v' for $v' \rightarrow \infty$, provided

^{*}brandenb@nordita.org[†]nils.haugen@phys.ntnu.no[‡]NBabkovskaia@gmail.com

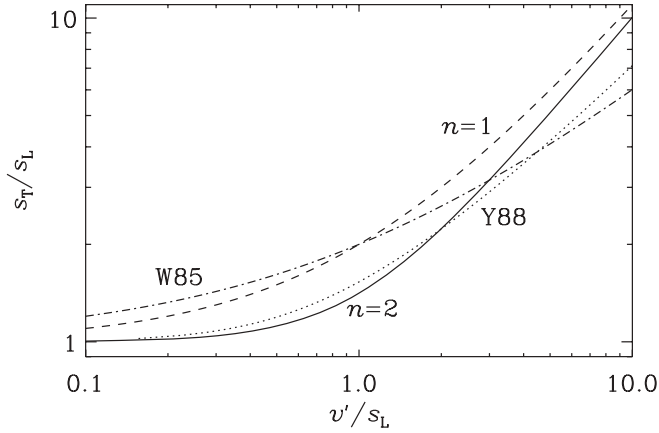


FIG. 1. Comparison of different expressions for the normalized front speed, s_T/s_L , as a function of the turbulent velocity, v'/s_L . The labels $n = 1$ and $n = 2$ refer to Eqs. (1) and (2), while Y88 and W85 refer to Eqs. (3) and (4).

$m < 1$ in Eq. (4). As can be seen from Fig. 1, the different proposals for the front speed are quite similar, making it difficult to use measurements to distinguish between them. Furthermore, realistic descriptions of flame properties are hampered by the fact that feedback on the flow by the actual combustion process depends on the specific case and is not easy to model. The feedback on the flow is therefore usually ignored. It might, therefore, be useful to return to a simple model of front propagation that can be treated in more detail and to address the unsettled question regarding the different proposals in Eqs. (1)–(4) for the dependence of s_T on v' . Following Kerstein [11], we consider here the Fisher equation, which is also known as the Kolmogorov-Petrovskii-Piskunov (KPP) equation [12]. An important difference from earlier work is the fact that we solve this equation in the three-dimensional case in the presence of a turbulent velocity field.

The Fisher or KPP equation is a simple scalar equation that possesses propagating front solutions. This equation is familiar in biomathematics [13] as a simple model for the spreading of diseases. It has also been amended by an advection term to describe the interaction with a turbulent velocity field in one [14] and multiple [15] dimensions, the effects of cellular flows [16], and the scaling of the front thickness [17]. Furthermore, the equation has also been modified to account for different interacting species, which can be used to model the spreading of autocatalytically polymerizing left- and right-handed nucleotides [18]. Given that C is a passive (albeit reacting) scalar, the Fisher equation does ignore any feedback on the flow and is therefore well-suited to help clarify questions regarding the relation between s_T and v' .

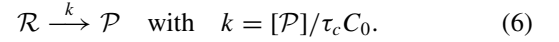
In the present paper, we consider both direct numerical simulations (DNS) of this equation in three dimensions as well as its averaged form where the effects of turbulence are being parametrized by a non-Fickian diffusion equation. Such an equation allows for the ballistic spreading of a passive scalar concentration on short time scales, which is expected to be important when the front propagates at a speed comparable to that of the turbulence itself.

II. THE FISHER EQUATION

A simple model of front propagation is the Fisher equation, which, in the simplest case, is a one-dimensional partial differential equation [12,13,19,20],

$$\frac{\partial C}{\partial t} = \frac{C}{\tau_c} \left(1 - \frac{C}{C_0}\right) + D \frac{\partial^2 C}{\partial x^2}, \quad (5)$$

for the concentration C . Here, τ_c is the chemical reaction time, D is the diffusivity, and C_0 is some saturation value above which further growth is quenched. Equation (5) corresponds to an autocatalytic reaction where a reactant \mathcal{R} yields a product \mathcal{P} at a rate k that is itself proportional to the concentration of the products, $[\mathcal{P}]$, that is,



This can then also be written as $\mathcal{P} + \mathcal{R} \rightarrow 2\mathcal{P}$. Saturation of the product concentration, $C = [\mathcal{P}]$, results from the fact that the total mass is conserved, that is, $[\mathcal{R}] + [\mathcal{P}] = C_0 = \text{const}$. The evolution equation for the concentration $C = [\mathcal{P}]$ is then given by Eq. (5).

This equation has two solutions: an unstable solution, $C = 0$, and a stable one, $C = C_0$. The diffusion term seeds the neighboring regions that are in an unstable state, which promotes the rapid transition from $C = 0$ to $C = C_0$. This leads to the propagation of the transition front in the direction down the gradient of C with a front speed [13]

$$s_L = 2\sqrt{D/\tau_c}, \quad (7)$$

where the subscript L refers to the *laminar* front speed.

In many cases of practical interest, the diffusion coefficient D is rather small and is hardly relevant when there is rapid advection through fluid motions. In that case, the governing equations become advection-reaction-diffusion equations. This can be written as

$$\frac{\partial C}{\partial t} + \nabla \cdot (\mathbf{U}C) = \frac{C}{\tau_c} \left(1 - \frac{C}{C_0}\right) + D \nabla^2 C, \quad (8)$$

where \mathbf{U} is the flow speed. If the flow is turbulent and has zero mean, there can be circumstances in which the average concentration \bar{C} can be described by an equation similar to Eq. (5), but with C being replaced by the mean value \bar{C} , and D being replaced by some turbulent diffusivity D_T , that is,

$$\frac{\partial \bar{C}}{\partial t} = \frac{\bar{C}}{\tau_c} \left(1 - \frac{\bar{C}}{C_0}\right) + D_T \frac{\partial^2 \bar{C}}{\partial x^2}, \quad (9)$$

where $D_T = D + D_t$ is the total (i.e., the sum of microscopic and turbulent) diffusivity. We have assumed here that the mean concentration shows a systematic variation in the x direction, and we have thus assumed averaging over the y and z directions, so $\bar{C}(x, t)$ can be described by a one-dimensional evolution equation.

Given the similarity between Eqs. (5) and (9), one would expect that in the turbulent case with appropriate initial conditions, the effective turbulent propagation speed s_T of the front can still be described by an expression similar to Eq. (7), but with D being replaced by D_T , that is, $s_T = 2\sqrt{D_T/\tau_c}$. A useful estimate for the turbulent diffusivity is $D_t = u_{\text{rms}}/3k_t$, where k_t is the wave number of the energy-carrying eddies

and u_{rms} is the rms velocity of the turbulence [21]. Thus, for $D_t \gg D$, the effective value of s_T is expected to be $2(u_{\text{rms}}/3\tau_c k_t)^{1/2}$. On the other hand, one cannot expect the front speed to increase indefinitely with decreasing τ_c . Indeed, one would not expect s_T to exceed the rms velocity of the turbulence in the direction of front propagation. Following common practice, we denote it by v' . Under the assumption of isotropy, v' is related to the three-dimensional rms velocity by $v' = u_{\text{rms}}/\sqrt{3}$.

An important nondimensional measure of τ_c is the Damköhler number, which is the ratio of the turnover time, $(u_{\text{rms}} k_t)^{-1}$, to τ_c . This number is defined here as

$$\text{Da} = (\tau_c u_{\text{rms}} k_t)^{-1}. \quad (10)$$

Note that our definition of Da is based on the *wave number* k_t rather than the *scale* $2\pi/k_t$, which would have reduced the numerical value of Da by a factor of 2π . For small values of Da, we expect $s_T \approx 2v' \text{Da}^{1/2}$, while for large values one expects $s_T \approx v'$ [8]. Thus, a more general formula is expected to be

$$s_T^2 = v'^2 f(\text{Da}), \quad (11)$$

where $f(\text{Da})$ increases linearly with Da for $\text{Da} \ll 1$ and $f(\text{Da}) \approx 1$ for $\text{Da} \gg 1$. This saturation behavior can also be interpreted as a reduction of the *effective* value of τ_c [22]. An important goal of this paper is to determine the form of the function $f(\text{Da})$.

III. NON-FICKIAN DIFFUSION

The Fickian diffusion approximation made in Eq. (9) for the mean concentration \bar{C} becomes invalid if \bar{C} varies rapidly in time, and in principle also in space. This is indeed expected to be the case when $\text{Da} \gg 1$. For rapid time variations, Eq. (9) attains then an extra time derivative and takes the form [23]

$$\tau \frac{\partial^2 \bar{C}}{\partial t^2} + \frac{\partial \bar{C}}{\partial t} = \frac{\bar{C}}{\tau_c} \left(1 - \frac{\bar{C}}{C_0}\right) + D_T \frac{\partial^2 \bar{C}}{\partial x^2}, \quad (12)$$

which is a damped wave equation with relaxation time τ and an additional reaction term. The presence of the nonlinearity in the reaction term leads to an additional contribution in the \bar{C} equation that has been ignored here (see Appendix for a more consistent treatment).

Without the reaction term, Eq. (12) is also known as the telegraph equation. This equation emerges naturally when computing turbulent transport coefficients using the τ approximation [24]. Evidence for the existence of the wave term has been found from isotropic forced turbulence simulations [23]. A nondimensional measure of τ is given by the Strouhal number,

$$\text{St} = \tau u_{\text{rms}} k_t = \tau u_{\text{rms}}^2 / 3D_t, \quad (13)$$

where the first equality is useful for turbulence simulations where $\tau u_{\text{rms}} k_t$ is readily evaluated, while the second equality is useful for the mean-field model, where k_t does not appear explicitly and D_t and u_{rms} are given.

Using DNS of forced turbulence with a passive scalar, the value of St has been determined to be around 3 by relating triple corrections to quadratic ones [23]. Although we consider the

value of St as being fairly well constrained, we do consider later a range of different values.

The purpose of this section is to study solutions of Eq. (12) that can then be compared with DNS of the Fisher equation coupled with the Navier-Stokes equations for obtaining a turbulent velocity that enters Eq. (8). We consider first the case in which D is negligible and we solve Eq. (12) for different values of Da in a one-dimensional domain that was chosen long enough so that the front speed can be determined accurately enough. We use a numerical scheme that is second order in space and third order in time [25]. In some cases, a resolution of $2^{15} \approx 3 \times 10^4$ mesh points was necessary.

We study first the dependence of the front speed on Da for a range of different values of St and $D \ll D_t$. Here, s_T is determined by differentiating the concentration integrated over the whole domain,

$$s_T(t) = \frac{d}{dt} \int \frac{\bar{C}}{C_0} dz, \quad (14)$$

and approximating the asymptotic front speed with the value at the time when the front has reached the other end of the domain. This quantity is also known as the reaction speed. This is indicated by \bar{C} reaching a small fraction (e.g., 10^{-6}) of C_0 . The result is shown in Fig. 2. For small values of Da, the front speed is independent of the value of St and we reproduce the anticipated result, that is, $f(\text{Da}) = 4 \text{Da}$. For larger values of Da, the front speed reaches eventually a constant value. However, the limiting value depends on St. Our results are well reproduced by the fit formula

$$\frac{s_T^2}{v'^2} \equiv f(\text{Da}, \text{St}) \approx \frac{4 \text{Da}}{1 + 3 \text{St Da}}. \quad (15)$$

This formula obeys the anticipated limiting behaviors for small and large values of Da, provided $\text{St} \approx 4/3$. The numerically determined data agree quite well with Eq. (15). However, in some cases the numerical data are somewhat uncertain and depend also slightly on resolution and domain size.

In the DNS presented below, where the numerical resolution is still limited, the value of D is often not negligible. Its value is characterized by the Peclet number,

$$\text{Pe} = u_{\text{rms}} / D k_t \approx 3D_t / D. \quad (16)$$

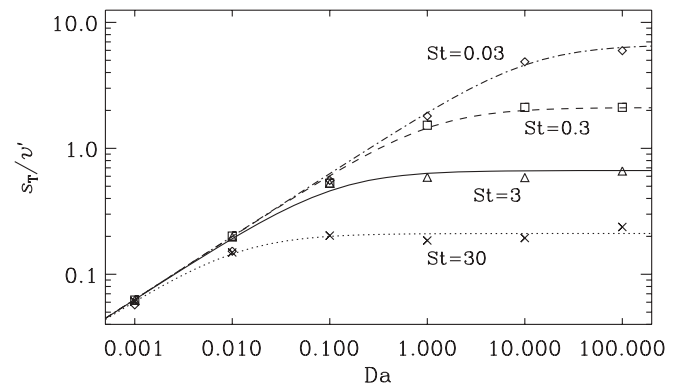


FIG. 2. Dependence of the front speed of solutions of Eq. (12) on Da for different values of St and $\text{Pe} = \infty$. The lines represent fits given by Eq. (15).

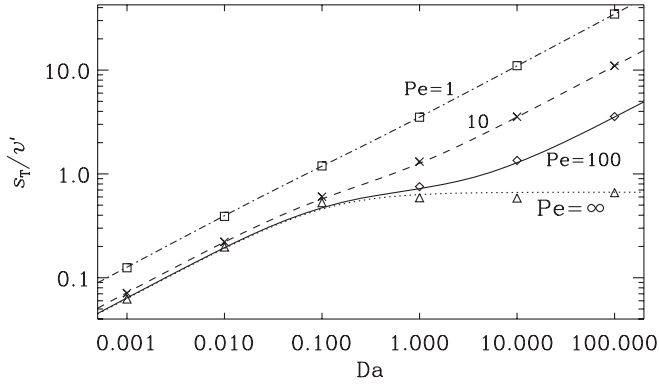


FIG. 3. Dependence of the front speed of solutions of Eq. (12) on Da for different values of Pe and $St = 3$. The lines represent fits given by Eq. (18).

For small values of Da , the expression for the front speed should be $s_T = 2\sqrt{(D_t + D)/\tau_c}$. Using $D_t = u_{rms}/3k_t$ and $v' = u_{rms}/\sqrt{3}$, together with the definitions Eqs. (10) and (16) for Da and Pe , respectively, we can express the ratio s_T/v' as

$$s_T/v' = 2\sqrt{(1 + 3Pe^{-1})Da} \quad (\text{for } Da \ll 1). \quad (17)$$

For larger values of Da we solve Eq. (12) numerically. A good fit formula for f is given by

$$f(Da, St, Pe) \approx 4Da \left(\frac{3}{Pe} + \frac{1}{1 + 3StDa} \right). \quad (18)$$

Note that f increases linearly with Da for small $Da \ll (3St)^{-1} \ll 1/9$ and also for intermediate values of Pe with $3 \ll Pe \ll 9StDa$. On the other hand, when both Da and Pe are large, with $3 \ll 9StDa \ll Pe$, we have $f = 4/3St = \text{const}$. In Fig. 3, we compare the fit formula with the numerically obtained front speeds for different values of Pe , keeping $St = 3$. The agreement is again quite good.

In turbulent combustion, it is customary to plot the normalized front speed, s_T/s_L , as a function of the normalized turbulent velocity, v'/s_L . Using our definitions of Da and Pe in Eqs. (10) and (16), respectively, we have $v'/s_L = (Pe/12Da)^{1/2}$ and find

$$\frac{s_T}{s_L} = \left[1 + \frac{1}{3St/4 + \epsilon v'/s_L} \left(\frac{v'}{s_L} \right)^2 \right]^{1/2}, \quad (19)$$

where we have defined $\epsilon = k_t \ell_F$, with $\ell_F = (\tau_c D/12)^{1/2}$ being a measure for the laminar flame thickness. Note that ϵ can also be expressed in terms of Da and Pe via

$$\epsilon = (12DaPe)^{-1/2}. \quad (20)$$

A more familiar quantity is the ratio $\ell/\ell_F = \epsilon^{-1}$, where $\ell = k_t^{-1}$ is the typical eddy scale. Even if we can assume the value of St to be given, ϵ is not a fixed quantity. It is therefore clear that there cannot be a unique relationship

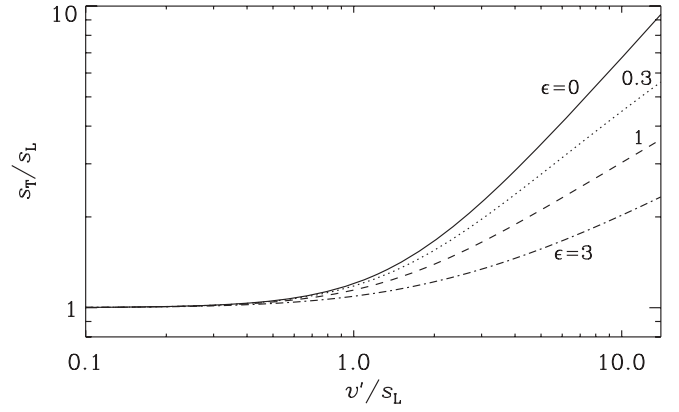


FIG. 4. Dependence of s_T/s_L and v'/s_L for $\epsilon = 0$ (solid line), 0.3 (dotted), 1 (dashed), and 3 (dash-dotted). Note that there is no unique relationship between s_T/s_L and v'/s_L .

between s_T/s_L and v'/s_L . Instead, there must be a family of solutions depending on the value of ϵ ; see Fig. 4.

IV. DNS OF THE FISHER EQUATION

We now consider DNS of Eq. (8) where \mathbf{U} is obtained by solving the Navier-Stokes equation for an isothermal gas with a forcing term that is δ correlated in time. The forcing function consists of plane waves whose wave vector is random and its length is within a narrow window around some mean forcing wave number k_t . Since the gas is compressible and the density ρ is not constant, Eq. (8) now takes the form

$$\frac{\partial C}{\partial t} + \mathbf{U} \cdot \nabla C = \frac{C}{\tau_c} \left(1 - \frac{C}{C_0} \right) + \nabla \cdot \left(\rho D \nabla \frac{C}{\rho} \right), \quad (21)$$

which we solve together with the momentum and continuity equations,

$$\frac{\partial \mathbf{U}}{\partial t} = -\mathbf{U} \cdot \nabla \mathbf{U} - c_s^2 \nabla \ln \rho + \mathbf{f} + \mathbf{F}_{\text{force}}, \quad (22)$$

$$\frac{\partial \rho}{\partial t} = -\nabla \cdot \rho \mathbf{U}, \quad (23)$$

where $\mathbf{F}_{\text{force}} = \nu(\nabla^2 \mathbf{U} + \frac{1}{3} \nabla \nabla \cdot \mathbf{U} + 2\mathbf{S} \nabla \ln \rho)$ is the viscous force, $\mathbf{S} = \frac{1}{2}[\nabla \mathbf{U} + (\nabla \mathbf{U})^T] - \frac{1}{3} \mathbf{I} \nabla \cdot \mathbf{U}$ is the traceless rate of strain tensor, \mathbf{I} is the unit matrix, ν is the kinematic viscosity, and $c_s = \text{const}$ is the isothermal sound speed. The forcing function \mathbf{f} is of the form

$$\mathbf{f}(\mathbf{x}, t) = \text{Re}\{N \mathbf{f}_{k(t)} \exp[i\mathbf{k}(t) \cdot \mathbf{x} + i\phi(t)]\}, \quad (24)$$

where \mathbf{x} is the position vector. The wave vector $\mathbf{k}(t)$ and the random phase $-\pi < \phi(t) \leq \pi$ change at every time step. For the time-integrated forcing function to be independent of the length of the time step δt , the normalization factor N has to be proportional to $\delta t^{-1/2}$. On dimensional grounds it is chosen to be $N = f_0 c_s (k_t c_s / \delta t)^{1/2}$, where f_0 is a nondimensional forcing amplitude. The value of the coefficient f_0 is chosen such that the maximum Mach number stays below about 0.5. Here we choose $f_0 = 0.02$. We force the system with nonhelical transversal waves,

$$\mathbf{f}_k = (\mathbf{k} \times \mathbf{e}) / \sqrt{k^2 - (\mathbf{k} \cdot \mathbf{e})^2}, \quad (25)$$

TABLE I. Summary of the runs discussed in this paper.

Run	A	Re	Pe	Da	Ka	k_t/k_1	s_T/v'	s_T/s_L	v'/s_L	ℓ/ℓ_F
A1	1	117	117	0.2	14.6	5.0	0.97	7.50	7.75	15.0
A2	1	115	115	0.5	4.8	5.1	1.60	7.03	4.38	26.3
A3	1	122	49	1.6	3.6	5.1	2.33	3.77	1.61	30.4
A4	1	121	12	4.8	4.8	5.1	3.55	1.63	0.46	26.3
A5	1	120	4	15.9	3.6	5.1	7.29	1.16	0.16	30.3
B1	4	38	513	1.6	3.6	1.6	1.88	9.76	5.19	98.9
B2	2	41	164	4.9	3.6	1.6	2.21	3.69	1.67	98.8
B3	2	165	165	4.9	3.6	1.6	2.52	4.22	1.67	98.9
B4	2	41	16	4.9	36.4	1.6	2.80	1.47	0.53	31.3
B5	2	40	16	50.3	3.6	1.6	7.25	1.19	0.16	98.9

where \mathbf{e} is an arbitrary unit vector not aligned with \mathbf{k} ; note that $|\mathbf{f}_k|^2 = 1$.

In the x direction, we use periodic boundary conditions for \mathbf{U} and ρ and $\partial C/\partial x = 0$ for C , while we use periodic boundary conditions in the y and z directions. The simulations were performed with the PENCIL CODE [26], which uses sixth-order explicit finite differences in space and a third-order accurate time-stepping method [25].

For the calculations we use units where $k_1 = c_s = \rho_0 = 1$. However, most of the results are presented in an explicitly nondimensional form by normalizing with respect to relevant quantities such as the rms velocity of the turbulence or the turnover time. Our simulations are characterized by several nondimensional parameters. In addition to the values of Da and Pe, defined in Eqs. (10) and (16), respectively, there is the Schmidt number, $Sc = \nu/D$. In those cases in which the Damköhler number was large, we had to increase the value of D in order to resolve the flame front. This was done by decreasing Sc to values below unity. The degree of scale separation is given by the ratio k_t/k_1 .

V. RESULTS

In the following, we present results for the uniform aspect ratio, $A = L_x/L_y = 1$ with $k_t/k_1 = 5$ (series A), and $A = 2$ or 4 with $k_t/k_1 = 1.6$ (series B). Our runs of series A and B are summarized in Table I. The resolution in the y and z directions is always 256^2 mesh points, but it is larger in the x direction in runs where the aspect ratio A is larger than unity. In Fig. 5, we show the concentration C on the periphery of the computational domain at different times for $\tau_c = 3/c_s k_1$, which corresponds to $Da = 0.5$; see Table I.

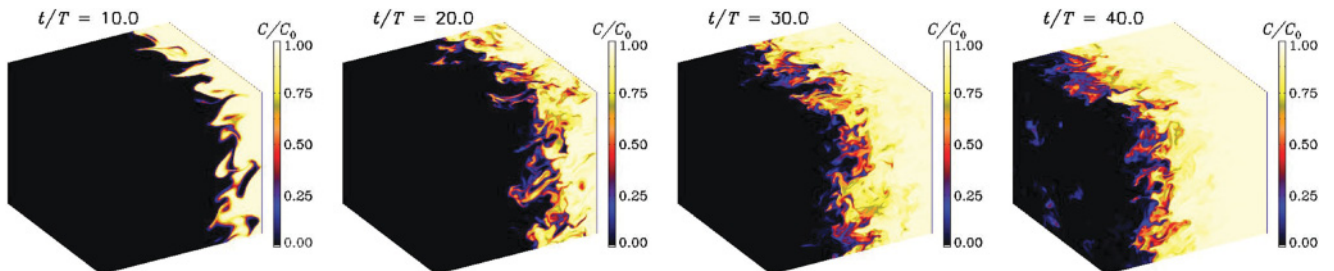


FIG. 5. (Color online) Visualization of the concentration C on the periphery of the box at different times for Run A2. Here, $T = (u_{rms} k_t)^{-1}$ is the turnover time.

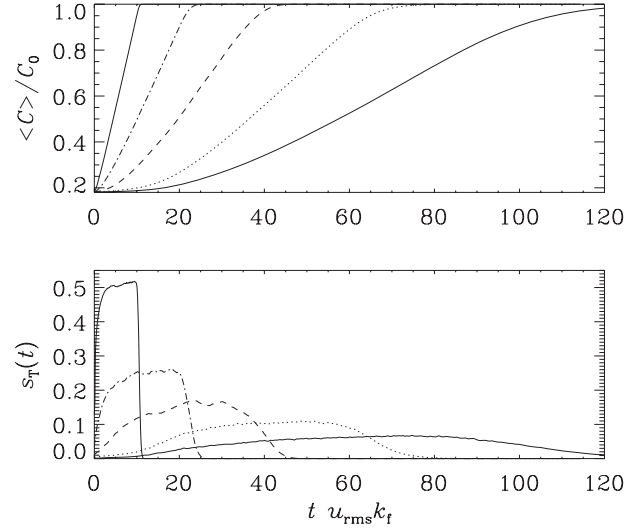


FIG. 6. Mean concentration and the instantaneous front speed as functions of time.

One sees clearly how the front spreads and propagates in the negative- x direction. The front speed is determined in the same way as for the mean-field model, that is, using Eq. (14), except that \bar{C} is computed from the actual C . This can also be formulated as a volume integral,

$$s_T(t) = \frac{1}{L_x L_y} \frac{d}{dt} \int \frac{C}{C_0} dV. \quad (26)$$

In Fig. 6, we show examples of the evolution of the mean concentration and the instantaneous front speed as functions of time for series A. The resulting ratios s_T/v' , s_T/s_L , v'/s_L , and ℓ/ℓ_F are summarized in Table I for series A and B.

In most of the cases considered in this paper, the value of Pe is not in the asymptotic regime. It might, therefore, be sensible to compare the relative front speed, s_T/v' , against the function $f(Da, St, Pe)$. This is done in Fig. 7, where we show the nondimensional front speed, s_T/v' , versus $f(Da, St, Pe)$, for three values of St using values of Da and Pe, as evaluated from Eqs. (10) and (16). Surprisingly, the best fit is obtained for rather small values of St of 0.03. This suggests that, for the present applications, the relevant value of τ is much smaller than in the case of a nonreacting passive scalar.

Next, we plot s_T/v' versus Da for different values of Pe; see Fig. 8 using the previously inferred value $St = 0.03$. The data points from the DNS tend to lie between the curves for $Pe = 1$ and 10, even though most of the actual values of Pe

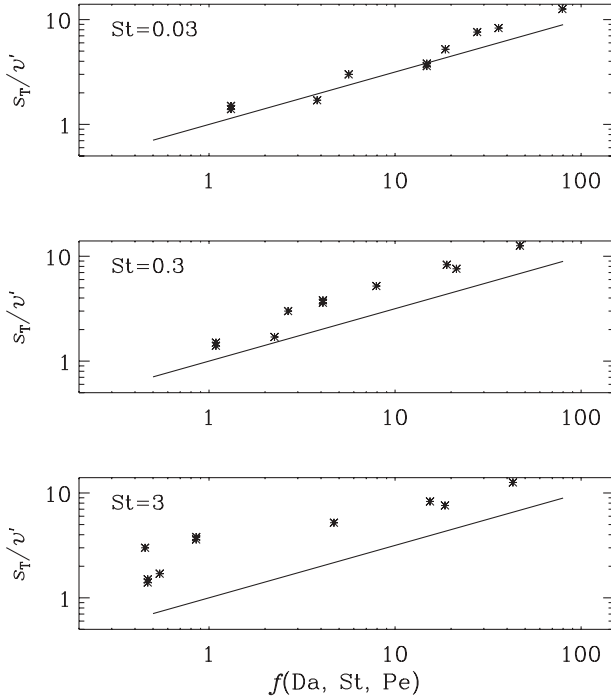


FIG. 7. Relative front speed as a function of f for three values of St . The squares indicate runs where the fluid is at rest and the front is moving through the domain, while the asterisks denote runs with an inlet velocity chosen such that the front is approximately stationary within the domain. The solid line gives the theoretically expected result, $s_T/v' = f(\text{Da}, \text{St}, \text{Pe})^{1/2}$. Note that the best agreement with the theoretical values is achieved for $St = 0.03$.

are beyond $\text{Pe} = 10$. This too suggests some inconsistency between the DNS and the mean-field description in terms of the telegraph equation. Finally, we plot the DNS results in a state diagram of s_T/s_L versus v'/s_L using $St = 0.03$; see Fig. 9. The data lie between the theoretical curves for $\ell/\ell_F = 10$ and 100, which is roughly in agreement with the values given in Table I.

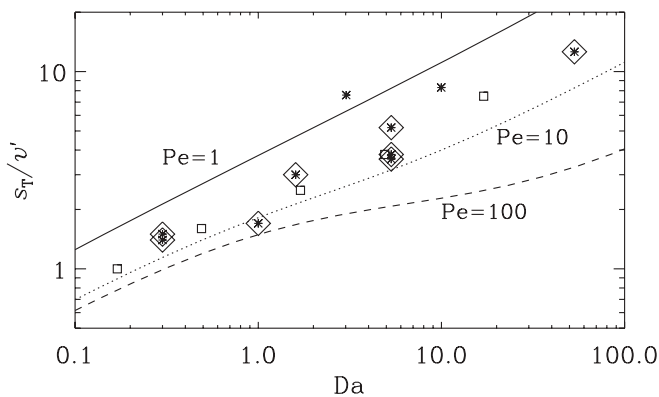


FIG. 8. Relative turbulent front speed vs Da . The squares indicate runs where the fluid is at rest and the front is moving through the domain, while the asterisks denote runs with an inlet velocity chosen such that the front is approximately stationary within the domain. For the latter, big asterisks denote cases in which $\text{Pe} > 10$. The lines give the theoretical expectations for $St = 0.03$ and $\text{Pe} = 1$ (solid line), 10 (dotted), and 100 (dashed line).

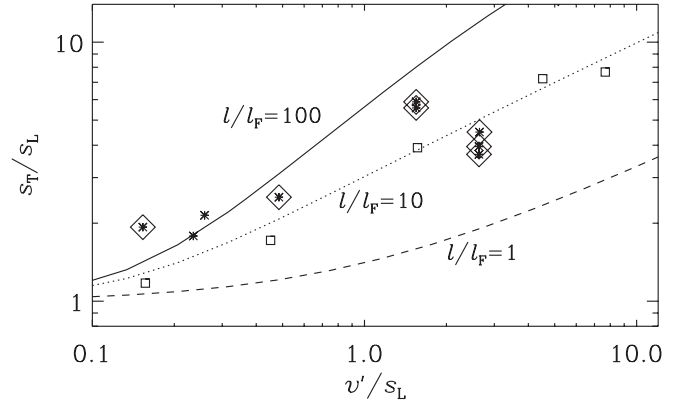


FIG. 9. Turbulent front speed vs turbulence intensity for $\epsilon = 0.1$ (solid line), 1 (dotted), and 10 (dashed) using $St = 0.03$. The squares indicate runs where the fluid is at rest and the front is moving through the domain, while the asterisks denote runs with an inlet velocity chosen such that the front is approximately stationary within the domain. For the latter, big asterisks denote cases in which $\text{Pe} > 10$. The lines give the theoretical expectations.

VI. CONCLUSIONS

In the present work, the Fisher equation has served as a simple model equation for front propagation in a turbulent flow. The model has similarities with turbulent combustion, but is much simpler. Nevertheless, it is clear that even this simple model harbors surprises that one might have overlooked under more complex conditions. Using three-dimensional simulations, we have been able to compare with the associated mean-field model. For small Damköhler numbers, the effective front speed can be approximated by replacing the diffusivity by a turbulent value. However, for Damköhler numbers larger than unity, this simple procedure fails, because it would suggest front speeds that exceed the characteristic speed of the turbulent eddies. A simple remedy is then to use a non-Fickian diffusion law for the turbulent diffusion and to retain the time derivative in the expression for the concentration flux. Earlier work [23] did already confirm the principal validity of this approach and resulted in an estimate for the relevant relaxation time, which is characterized by the Strouhal number. The current work shows that the best fit to the simulation data can be achieved with a Strouhal number that is as small as 0.03, which is about 100 times smaller than the earlier-determined value for passive scalar diffusion in forced turbulence. This difference is connected with the presence of a reaction term in the evolution equation for the passive scalar concentration.

ACKNOWLEDGMENTS

We thank an anonymous referee for making useful suggestions. We are also grateful to the participants of the Nordita program on turbulent combustion in May, 2010, when this paper was written, for providing a stimulating atmosphere. We acknowledge the allocation of computing resources provided by the Swedish National Allocations Committee at the Center for Parallel Computers at the Royal Institute of Technology in Stockholm and the National Supercomputer Centers in Linköping. This work was supported in part by the European Research Council under the AstroDyn Research

Project 227952, the Swedish Research Council Grant No. 621-2007-4064, and the European Community's Seventh Framework Programme (FP7/2007-2013) under Grant Agreement No. 211971 (The DECARBit project) (NELH).

APPENDIX: MEAN-FIELD EFFECT OF THE REACTION TERM

In order to assess the effect of neglecting the reaction term in the analysis presented earlier, we present now a simple mean-field theory for the Fisher equation using the τ equation. We start with the passive scalar equation with a reaction term as given by Eq. (8), split $C = \bar{C} + c$ and $\mathbf{U} = \bar{\mathbf{U}} + \mathbf{u}$ into mean and fluctuating parts, neglect the molecular diffusion term for simplicity, and define the mean concentration flux $\bar{\mathcal{F}} = \overline{\mathbf{u}c}$ and the mean-squared concentration, $\bar{\mathcal{H}} = \overline{c^2}$, so the equation for the mean concentration is

$$\frac{\partial \bar{C}}{\partial t} = -\nabla \cdot (\bar{\mathbf{U}} \bar{C} + \bar{\mathcal{F}}) + \frac{\bar{C}}{\tau_c} \left(1 - \frac{\bar{C}}{C_0}\right) - \frac{\bar{\mathcal{H}}}{\tau_c C_0}, \quad (\text{A1})$$

so the equation for the fluctuations is, to linear order in the fluctuations,

$$\frac{\partial c}{\partial t} = -\nabla \cdot (\bar{\mathbf{U}} c + \mathbf{u} \bar{C}) + \frac{c}{\tau_c} \left(1 - \frac{2\bar{C}}{C_0}\right) + \dots, \quad (\text{A2})$$

where the dots denote higher-order terms for which we shall adopt a general closure assumption. Next, we derive evolution equations for $\bar{\mathcal{F}}$ and $\bar{\mathcal{H}}$, ignore a mean flow for simplicity, and assume $\nabla \cdot \mathbf{u} = 0$, so we have

$$\frac{\partial \bar{\mathcal{F}}}{\partial t} = -\tilde{D}_t \nabla \bar{C} + \frac{\bar{\mathcal{F}}}{\tau_c} \left(1 - \frac{2\bar{C}}{C_0}\right) - \frac{\bar{\mathcal{F}}}{\tau}, \quad (\text{A3})$$

$$\frac{\partial \bar{\mathcal{H}}}{\partial t} = -2\bar{\mathcal{F}} \cdot \nabla \bar{C} + 2\frac{\bar{\mathcal{H}}}{\tau_c} \left(1 - \frac{2\bar{C}}{C_0}\right) - \frac{\bar{\mathcal{H}}}{\tau}. \quad (\text{A4})$$

In Eqs. (A3) and (A4), we can write the last two terms as $-\bar{\mathcal{F}}/\tau_{\mathcal{F}}$ and $-\bar{\mathcal{H}}/\tau_{\mathcal{H}}$, respectively, where

$$\frac{1}{\tau_{\mathcal{F}}(\bar{C})} = \frac{1}{\tau} - \frac{1}{\tau_c} \left(1 - \frac{2\bar{C}}{C_0}\right), \quad (\text{A5})$$

$$\frac{1}{\tau_{\mathcal{H}}(\bar{C})} = \frac{1}{\tau} - \frac{2}{\tau_c} \left(1 - \frac{2\bar{C}}{C_0}\right). \quad (\text{A6})$$

TABLE II. Dependence of s_T/v' without and with $\bar{\mathcal{H}}$ in a model for $Pe = 10$. Note the slight increase of s_T/v' in the presence of $\bar{\mathcal{H}}$ compared to the case in which it is neglected.

Da	s_T/v' (without $\bar{\mathcal{H}}$)	s_T/v' (with $\bar{\mathcal{H}}$)
0.10	0.25	0.25
0.30	0.44	0.47
0.50	0.59	0.65
0.61	0.66	0.73

On sufficiently long time scales we may ignore the time derivatives in Eqs. (A3) and (A4), so we arrive at closed expressions for $\bar{\mathcal{F}}$ and $\bar{\mathcal{H}}$, which we insert into Eq. (A1), to obtain

$$\frac{\partial \bar{C}}{\partial t} + \mathbf{U}_c \cdot \nabla \bar{C} = \frac{\bar{C}}{\tau_c} \left(1 - \frac{\bar{C}}{C_0}\right) + D_T \nabla^2 \bar{C}, \quad (\text{A7})$$

where $\mathbf{U}_c(\bar{C})$ is a new effective advection speed and $D_T = D + D_t$ is again the sum of turbulent and microscopic diffusivities with

$$\mathbf{U}_c(\bar{C}) = 2D_t \frac{\tau_{\mathcal{H}}}{\tau_c} \frac{\nabla \bar{C}}{C_0}, \quad D_t(\bar{C}) = \tau_{\mathcal{F}}(\bar{C}) v'^2. \quad (\text{A8})$$

One may expect that the term \mathbf{U}_c slows down the propagation speed of the front, because it is directed up the concentration gradient. Note that the sign of the \mathbf{U}_c term is opposite to that of a similar term in the so-called G equation [2,10] of turbulent front propagations, which is, however, not an equation for the flame brush but for the detailed position of the wrinkled flame front (at $G = 0$) with an advection speed that is given by $\mathbf{u} - s_L \hat{\mathbf{n}}$, where $\hat{\mathbf{n}} = \nabla G / |\nabla G|$ is a unit vector normal to the flame front, but it enters with a minus sign and thus corresponds to an enhanced speed down the gradient of G . However, by solving Eq. (A1) with Eqs. (A3) and (A4), it turns out that when the $\bar{\mathcal{H}}$ term is included, it accelerates the front; see Table II. Note also that the coefficient D_t is reduced and can even become negative in the unstable part of the front where $C = 0$ (or at least $C < C_0/2$); see Eqs. (A5) and (A8). In that case our expression for turbulent diffusion becomes invalid and one has to include higher-order derivatives that would guarantee stability at small length scales.

[1] G. Damköhler, *Elektrochem. Angew. Phys. Chem.* **46**, 601 (1940).
 [2] N. Peters, *J. Fluid Mech.* **384**, 107 (1999).
 [3] R. W. Bilger, S. B. Pope, K. N. C. Bray, and J. F. Driscoll, *Proc. Combust. Inst.* **30**, 21 (2005).
 [4] J. F. Driscoll, *Prog. Energy Comb. Sci.* **34**, 91 (2008).
 [5] H. Kido, M. Nakahara, K. Nakashima, and J. Hashimoto, *Proc. Combust. Inst.* **29**, 1855 (2002).
 [6] V. R. Savarianandam and C. J. Lawn, *Combust. Flame* **146**, 1 (2006).
 [7] T. Kitagawa, T. Nakahara, K. Maruyama, K. Kado, A. Hayakawa, and S. Kobayashi, *Int. J. Hydrogen Energy* **33**, 5842 (2008).
 [8] A. Pocheau, *Europhys. Lett.* **20**, 401 (1992).

[9] V. Yakhot, *Combust. Sci. Technol.* **60**, 191 (1988).
 [10] F. A. Williams, *Combustion Theory* (Addison-Wesley, Reading, PA, 1985).
 [11] A. R. Kerstein, *Proc. Combust. Inst.* **29**, 1763 (2002).
 [12] A. N. Kolmogorov, I. G. Petrovskii, and N. S. Piskunov, *Moscow Univ. Bull. Math.* **1**, 1 (1937).
 [13] J. D. Murray, *Mathematical Biology. An Introduction* (Springer, New York, 2002).
 [14] R. Benzi and D. R. Nelson, *Physica D* **238**, 2003 (2009).
 [15] P. Perlekar, R. Benzi, D. R. Nelson, and F. Toschi, *Phys. Rev. Lett.* **105**, 144501 (2010).
 [16] M. Cencini, A. Torcini, D. Vergni, and A. Vulpiani, *Phys. Fluids* **15**, 679 (2003).

- [17] S. Berti, D. Vergni, and A. Vulpiani, *Europhys. Lett.* **83**, 54003 (2008).
- [18] A. Brandenburg and T. Multamäki, *Int. J. Astrobiol.* **3**, 209 (2004).
- [19] R. A. Fisher, *Ann. Eugenics* **7**, 353 (1937).
- [20] P. Kaliappan, *Physica D* **11**, 368 (1984).
- [21] A. Brandenburg, A. Svedin, and G. M. Vasil, *Mon. Not. R. Astron. Soc.* **395**, 1599 (2009).
- [22] T. Elperin, N. Kleeorin, and I. Rogachevskii, *Phys. Rev. Lett.* **80**, 69 (1998).
- [23] A. Brandenburg, P. Käpylä, and A. Mohammed, *Phys. Fluids* **16**, 1020 (2004).
- [24] E. G. Blackman and G. B. Field, *Phys. Fluids* **15**, L73 (2003).
- [25] A. Brandenburg and W. Dobler, *Comp. Phys. Commun.* **147**, 471 (2002).
- [26] The PENCIL CODE is a high-order finite-difference code (sixth order in space and third order in time) for solving the compressible magnetohydrodynamics equations [<http://pencil-code.googlecode.com>].